SEISMIC PERFORMACE OF ARC-WELDED STEEL PIPES FOR WATER LIFELINES

T. Imai
JFE Engineering Corporation,Yokohama, Japan

T. Koike
Kyoto University, Kyoto, Japan

SUMMARY:
The seismic performance of arc-welded steel pipes was examined in a full-scale compression experiment to obtain the critical strains for the ultimate and repairable limit states which should be used for the performance-based seismic design of water lifelines. Based on the experimental results, a new performance-based seismic design method for arc-welded thin-wall steel pipes used for water lifelines is proposed.

Keywords: performance-based design, arc-welded steel pipe, seismic performance, water pipeline

1. GENERAL INSTRUCTIONS

The seismic performance of the lifeline system should be related to the limit states of the system, which can be described as the serviceability limit state, the repairable limit state, and the ultimate limit state for the corresponding seismic disasters.
Water leakage failure caused by crack extension from a buckled portion of a thin-wall steel pipe in a seismic event is a typical example of the ultimate limit state of water lifelines. In view of steel pipe failure modes, the current seismic design guideline for water pipelines in Japan requires assessment of seismic strain not exceeding the critical strain initiating local buckling when the large ground motion by the Maximum Considered Earthquake (MCE) is given. However, this criterion is not adequate for an MCE which requires assessment of the ultimate limit state. This is due to the present inadequate situation, in which crucial data on the structural strains of thin-wall steel pipes are not available for these limit states.
The seismic performance of arc-welded steel pipes was examined in a full-scale compression experiment in order to obtain the critical strains for the ultimate and repairable limit states which should be used for the performance-based seismic design of water lifelines. From this full-scale experiment, the strain initiating the first buckling deformation was obtained as the critical strain for the repairable limit state. The strain producing leakage failure from the buckled portion was also measured as the critical strain for the ultimate limit state.
Based on the experimental results, a new performance-based seismic design method for arc-welded thin-wall steel pipes used for water lifelines is proposed. The seismic performance for the ultimate limit state is assessed by the low-cycle fatigue approach for seismic ground motions, and also by the pipe restrained length approach for permanent ground displacements such as liquefaction and landslide. The numerical results of the seismic assessment show that arc-welded steel pipes have sufficient strength for these seismic loads.

2. SEISMIC PERFORMANCE-BASED DESIGN OF WATER PIPLINES

2.1. Seismic Performance of Water Pipelines

2.1.1 Current definition of seismic performance of water pipelines

The current design guideline (JWWA 1997 & 2009, AHLW 2008) in Japan specifies the two types of seismic performance for the water pipes which are classified into two groups these being steel pipes with arc-welded joints and ductile cast iron pipes with mechanical joints. Important facilities including pipe bridges (Ohuchi 2008), storage reservoirs and pumping equipment are also required to have higher seismic performance than ordinary structural components, including pipes, which are used in distribution lines. After the 1995 Kobe Earthquake, two types of seismic loads, Level 1 and Level 2 ground motions, which correspond to the maximum operational earthquake (MOE) and the maximum considered earthquake (MCE), were introduced for use in seismic safety assessments. Table 1 shows the seismic performances which are classified for the serviceability limit state and the repairable limit state. However, there is no description of the ultimate limit state in the current seismic design guideline. Also, the critical strains are given as the allowable pipe strains in Table 2, in which two equations are derived from the theoretical formula 57.5t/D (%) for the first buckling strain of a thin-wall cylinder with a safety factor of 2 for Level 1 ground motion and a safety factor of 1.25 for the Level 2 ground motion, respectively (WSP 1996).

Table 1 Current seismic performance and their limit states of various water pipelines.

Pipe joint system		Seismic performance		
		Performance 1	Performance 2	Performance 3
Joint type	Component type	Serviceability limit state	Repairable limit state	Ultimate limit state
Arc-welded joint	Continuous pipe	Pipe stress in the elastic region	Partially inelastic, but no leakage	None
Mechanical joint	Pipe body	Pipe stress in the elastic region	Pipe stress in the elastic region	None
	Joint	Joint in the allowable range	No leakage from the joint	None

Table 2 Allowable pipe strains in the current design guideline.

Ground motion	Acceptable strain ε_a (%)
Level 1	$23 \cdot \frac{t}{D}$
Level 2	$46 \cdot \frac{t}{D}$

2.1.2 Proposed seismic performance

The current design guideline in Japan has assumed that seismic performance 2 (repairable limit state), meaning seismic damage that can be repaired within a few days, is the severest limit state for a pipeline and it is not necessary to secure seismic performance 3 (ultimate limit state), meaning seismic damage restoration requiring more than one month. However, recent earthquakes have necessitated the introduction of seismic performance 3 in order to be applicable to the actual damage situation in Japan. Actually, in recent severe earthquakes such as the 2007 Niigata-ken Chuetsu-oki Earthquake (Niigata Prefecture Chuetsu Offshore Earthquake) and the 2011 Great East Japan Earthquake, restoration required more than one month. From these observations, seismic performance 3 must be introduced to describe a limit state which is related to ultimate damage and its corresponding restoration requiring more than several months.

In this situation, Table 1 can be revised as Table 3 by adding seismic performance 3.

In Table 3, a mechanical joint without a locking system is easily pulled out when a relative displacement forced by Level 2 ground motion exceeds the allowable limit. This means that a mechanical joint without a locking system intrinsically lacks seismic performance 2 and 3. For comparison among the three different types of joint system, however, this joint is included in Table 3. Table 4 shows the safety assessment criteria for the three seismic performances or limit states.

Table 3 Proposed seismic performances and their limit states of various water pipelines.

Pipe joint system		Seismic performance		
		Performance 1	Performance 2	Performance 3
Limit state		Serviceability limit state	Repairable limit state	Ultimate limit state
Arc-welded	Continuous pipe	Pipe stress in the elastic region	Partially inelastic, but no leakage	No leakage from the bending corner of the buckled pipe
Mechanical joint	Pipe body	Pipe stress in the elastic region	Pipe stress in the elastic region	Pipe stress in the elastic region
	Joint without a locking system	Each joint in the allowable range	Seismic response to be absorbed by one joint with a sufficient allowance, and no leakage from the joint	Seismic response to be absorbed by one joint without any allowance, but no leakage from the joint
	Joint with a locking system	Each joint in the allowable range	Seismic response to be absorbed by multiple joints with a sufficient allowance, and no leakage from the joint	Seismic response to be absorbed by multiple joints w/o any allowance, but no leakage from the joint

Table 4 Proposed seismic safety assessment criteria of various water pipelines.

Pipe joint system		Seismic performance & limit state		
		Performance 1	Performance 2	Performance 3
		Serviceability limit state	Repairable limit state	Ultimate limit state
Pipeline ranking	for Level 1 ground motion	Rank A1& A2	Rank B	None
	for Level 2 ground motion	None	Rank A1 & A2	Rank A2
Arc-welded	Continuous pipe	$\sigma_p \le \sigma_y$ or $\varepsilon_p \le \varepsilon_y$	$\varepsilon_y \le \varepsilon_p \le \varepsilon_{cr}^{repair}$	$\varepsilon_{cr}^{repair} \le \varepsilon_p \le \varepsilon_{cr}^{ultimate}$
Mechanical joint	Pipe body	$\sigma_p \le \sigma_y$		
	Joint w/o a locking system	$\delta_J \le \delta_{cr}$		
	Joint with a locking system	$\delta_J \le \delta_{cr}$	$\delta_J \le n\delta_{cr}$	$\delta_J \le n_{\max}\delta_{cr}$

Note: Rank A1: important facility, Rank A2: very important facility and Rank B: standard facility
δ_J : relative displacement between the pipe and the joint of a pipeline with a mechanical joint,
$n, n_{\max}, \delta_{cr}$: number of joints, the maximum number of joints, critical displacement of a joint,
$\sigma_p, \varepsilon_p, \sigma_y, \varepsilon_y, \varepsilon_{cr}^{repair}, \varepsilon_{cr}^{ultimate}$: stress and strain of a pipe, yield stress and strain of a pipe, critical strains for the repair and ultimate limit states, respectively.

3. FULL-SCALE BUCKLING EXPERIMENT WITH THE THIN-WALL CYLINDER SIMULATING WATER PIPELINES

3.1. Experimental Method

Figure 1 is a side view of the test pipe, which is reinforced at both ends, so that buckling occurs in the middle portion of the cylinder. This experiment is performed to obtain the ultimate limit state criterion of a thin-wall steel cylinder for water pipelines. Three test pieces with the dimensions given in Table 5 and 6 are used in this experiment.

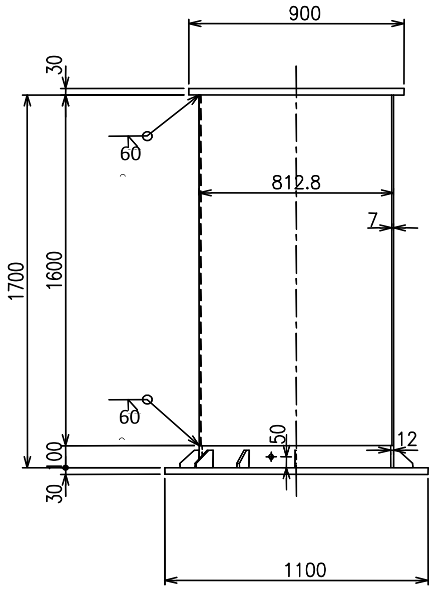

Figure 1 Side view of test pipe.

Table 5 Dimensions of test pipes.

Test pipe	Diameter (mm)	Thickness (mm)	***D / t***
Pipe-1	809.4	7.45	109
Pipe-2	810.6	7.28	111
Pipe-3	812.7	7.24	112

Table 6 Tensile test results of specimens taken from test pipes

Test Pipe	Cross section (mm^2)	Yield stress (N/mm^2)	Tensile strength (N/mm^2)	Max. elongation (%)
Pipe-1	221.8	286.7	424.7	29.0
		280.9		
Pipe-2	220.8	327.4	439.3	30.1
		317.9		
Pipe-3	220.8	327.4	439.3	30.1
		317.9		

3.2. Buckling Behaviors

Photo 1 to Photo 6 show the progressive process of buckling formation in a thin-wall steel cylinder under compression loading. Since the diameter/thickness ratio, *D/t* is approximately 110, buckling deformation starts from the wrinkling formation of Photo 1. After sticking of the wrinkle in Photo 2, a second wrinkle is produced in Photo 3. In the next step, a complex wrinkling behavior appears in Photo 4, and deformation continues until the third buckling mode is reached in Photo 5. The final deformation in Photo 6 is obtained by repetition of the same process.

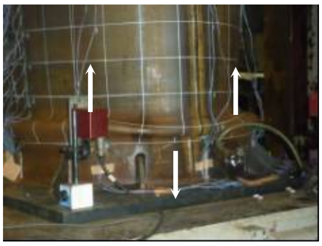

Photo 1 STEP1: Formation of a buckling wrinkle.

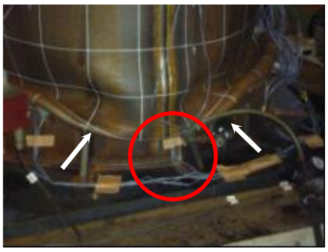

Photo 2 STEP2: Sticking of the wrinkle to the pipe.

Photo 3 STEP3: Formation of a 2nd wrinkle.

Photo 4 STEP4: Sticking of wrinkle to the pipe (3rd wrinkle is formed).

Photo 5 STEP5: Final deformation condition.

Photo 6 STEP5: End view of the deformed pipe.

3.3. Crack Initiation from Buckled Corner

Figures 2 and 3 show the process of repeated compression loading for axial displacements to obtain a crack or the maximum deformation limit. In test pipe 1, repeated compression loading was stopped at the 7th repetition, which corresponded to the maximum stroke of the loading machine (828 mm). Test pipe 2 showed leakage in the unloading stage of the 4th repetition of compression loading. The crack formation (Goto 1997) in the buckled portion appeared inside the red circle in Photo 7. Test pipe 3, on the other hand, showed a different behavior, in which buckling appeared after the first compression and the crack was also formed in the unloading stage of this loading process. The crack in test pipe 2 might be explained by the observation that crack extension was delayed because deformation was restrained by the superimposed buckling layers. The early leakage in test pipe 3 can also be explained by the observation that the surrounding deformation condition allowed free crack extension.

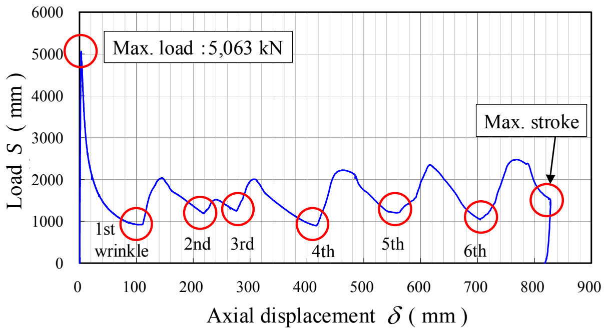

Figure 2 Axial deformation process of test pipe 1.

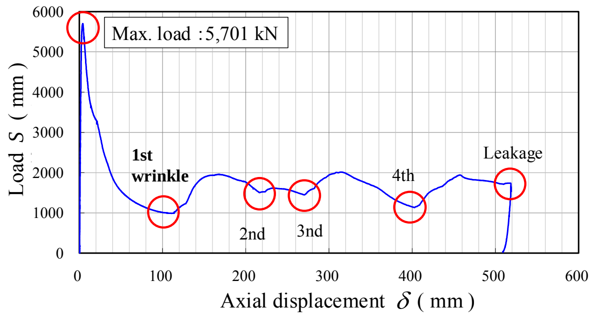

Figure 3 Axial deformation process of test pipe 2.

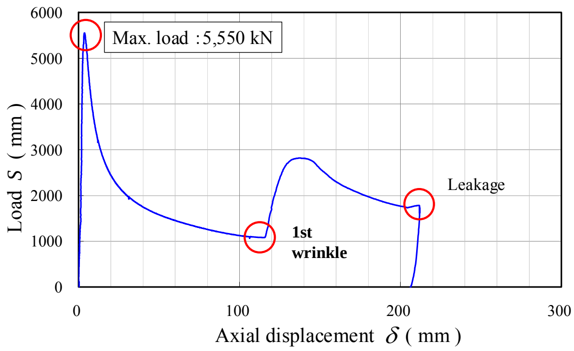

Figure 4 Axial deformation process of test pipe 3.

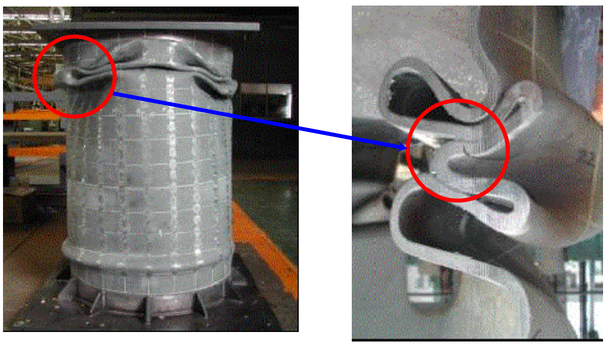

Photo 7 Crack initiating portion of test pipe 2.

3.4. Seismic Performance Analysis of Arc-welded Steel Pipes

The critical strains for the Level1 and Level2 ground motions in the current design guidelines are the critical strain initiating local buckling, which was derived from buckling experiments of thin-wall steel cylinders (ASME 1997). This strain does not always correspond to the strain for leakage. Since there is some amount of difference between these two strains, the current seismic design guideline keeps a sufficient safety allowance for leakage failure from the buckling mode.
The following subsection will provide the critical strains for the proposed seismic performances.

3.4.1 Buckling initiation strain
Figure 5 is the stress and strain diagram superimposed for three test results which show the Round House type of steel pipe material. Each maximum strain corresponds to the buckling initiation strain measured in the experimental observations. In Table 7, the buckling strains measured in this experiment are compared with those of the Equation (1), which was proposed by Kato and et al. (1973).

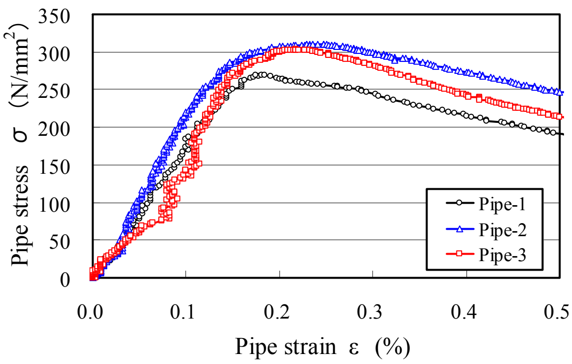

Figure 5 Stress-strain curves for test pipes.

Table 8 Buckling strains for test pipes.

Test pipe	Max.load (kN)	Displacement (mm)	Buckling strain (%)	
			Experim-ental data	Eq(1)
Pipe-1	5,063	3.4	0.200	0.390
Pipe-2	5,701	4.4	0.259	0.401
Pipe-3	5,550	4.4	0.259	0.397

$$\varepsilon_B = \frac{4}{3} \cdot \sqrt{m} \cdot \frac{t}{D_m} \quad (1)$$

in which D_m, m, t are the mean diameter of the pipe, the strain hardening index (Kato and et al. 1973) of 0.11, and the pipe wall thickness, respectively.

The difference between the experimental result and theoretical results depends on the difference of the pipe material and the pipe fabrication method. The equation developed by Kato and et al. was based on mild steel materials for structural use, STK 41 and STK 50 in JIS code (2007), with fabricating by the electric seaming method, whereas the test pipe in this study was mild steel material for pipe use, STPY 400 fabricated by the plate bending method.

3.4.2 Axial compression strain at the buckling initiation

According to the detailed observation of crack formation to leakage shown in Figures 3 and 4, superimposed buckling layers can retard the development of crack extension. Therefore, the leakage initiation process from crack formation can be summarized as (1) first buckling formation, (2) buckling layer formation, (3) superimposition of the buckled layers, (4) surface crack formation, and (5) through-crack formation.

Figure 6 shows the superimposed result of the three curves in Figures 2 to 4, in which the peak and tough locations of each process appear almost at the same axial displacement, but the number of repetition cycles varies depending on the structural and experimental conditions.

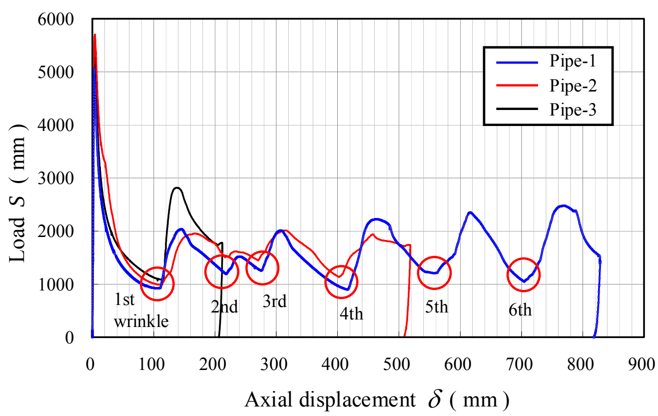

Figure 6 Axial deformation process for all pipes

3.4.3 Relationship among buckling profile, bucking corner and crack initiation strain

Figure 7 is a schematic profile of the buckled cross section after first buckling. The buckling width and height, L_w and L_h are given by several parameters derived from buckling theory (1961) as follows.

$$L_w = 1.72\sqrt{r \cdot t} \quad \text{(half wave length of a buckling)} \quad (2a)$$

$$L_h = s \cdot t \quad (2b)$$

in which r, t are the radius of the pipe and the pipe wall thickness, and n, s are geometrical parameters, respectively.

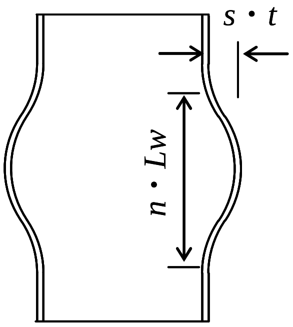

Figure 7 Buckling profile model.

Table 8 Buckling width of test pipes.

	Diameter	Thickness	Ratio of axial compression	Buckling width	
				Theory	Experiment
No.	D	t	e_W	L_W	$L_{wnominal}$
	mm	mm	%	mm	mm
Pipe-1	809.4	7.45	6.52	94.01	104.32
Pipe-2	810.6	7.28	6.66	93.01	106.56
Pipe-3	812.7	7.24	6.81	92.88	108.96

The axial displacement δ at the first buckling is located at almost the same point in the three test pipes as shown in Figure 6. From this observation, the ratio of axial compression can be defined as

$$e_W = \delta / H \tag{3a}$$

in which δ and H are the axial displacement at first buckling formation and the original height of the test pipe, respectively. Using this ratio, the buckling width can be approximately estimated as

$$L_{Wnominal} = H \cdot e_W \ . \tag{3b}$$

Two bucking widths, L_W and $L_{Wnominal}$, are compared in Table 8 where the theoretical value underestimates the experimental result by approximately 10%.

The local strain at the buckling corner for the axial displacement δ cannot be measured directly with strain gauges, so the FEM approach was adopted in this study. Based on the FEM code ADINA(1986) Ver 6.74, the strain distribution of the test pipe is obtained as shown in Figure 8. The maximum strain ε_U is approximately calculated as 35%. On the other hand, a three point bending test (based on the Japanese standard for the material experiment method, JIS Z2204 with 9 test specimen produced from the steel pipe was carried out. The obtained experimental statistical results were a mean value of 34.6% and its standard deviation of 12.9%.

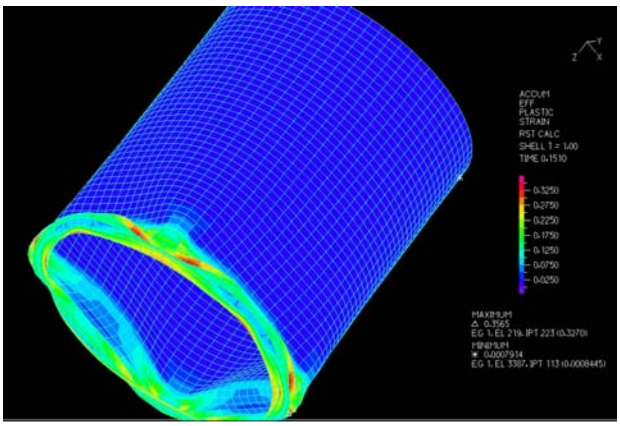

Figure 8 FEM analysis of test pipe for compression loading condition.

The buckling formation process by seismic load can be described in the following way:

(1) The seismic ground motion may produce the buckling initiation strain;

(2) The first wrinkle is formed with a width of L_W , and the maximum strain ε_U of 35% is created at the maximum curvature point, but no leakage occurs;

(3) After repetitions of seismic loading, the repeated strains may produce a fatigue crack at the maximum strain corner of the single wrinkle layer or can cause multiple wrinkle formation in which case several wrinkle layers are superimposed;

(4) When the fatigue crack develops to full penetration through the wall thickness, i.e., a through-crack, leakage occurs; or
(5) When the several wrinkle layers are in strong contact, a surface crack forms initially, and a penetrating crack will then develop at the weakest point.
In terms of this process, the repairable limit state corresponds to the stage of first wrinkle formation, and the ultimate limit state is the stage when formation of a penetrating crack results in leakage.

4. SEISMIC PERFORMANCE ASSESSMENT OF ARC-WELDED STEEL PIPE

4.1. Critical Strain for Seismic Design of Water Pipelines

The seismic design (Imai and Koike 2009) for water pipelines is developed for Level 2 ground motion, in which the effect of buckling wrinkle formation is taken into consideration.
Based on the previous discussion, the repairable limit state corresponds to the stage when the first wrinkle has been formed. Therefore, the probability of repairable failure is defined as

$$p_f^2 \equiv P\left[\varepsilon_W^2 \le \varepsilon_p \middle| EQ_2\right] \tag{4}$$

where ε_p is the seismic strain of the pipeline, and ε_W^2 is the critical strain for wrinkle formation given by

$$\varepsilon_W^2 = 1.25 \times 46 \frac{t}{D} = 57.5 \frac{t}{D} \quad (\%) \tag{5}$$

When a repeated strain increment $\Delta\varepsilon$ is loaded at the wrinkle point, a low cycle fatigue crack develops and may ultimately become a penetrating crack. The critical strain for this fatigue failure is given by the number of loading cycles N and the mean strain level ε_U by $\varepsilon_{F_{cr}}(N, \varepsilon_U)$. The strain increment is given by

$$\Delta\varepsilon = \frac{t^3 L_h}{2I} \varepsilon_p \tag{6}$$

Therefore, the probability of failure for the ultimate limit state or seismic performance 3 is defined as

$$p_f^3 \equiv P\left[\varepsilon_W^3 \le \Delta\varepsilon \middle| EQ_2\right] \tag{7}$$

in which

$$\varepsilon_W^3 = \frac{2I}{t^3 L_h} \varepsilon_{F_{cr}} \tag{8}$$

where L_h, I, t are the buckling height given by Equation (2b), the geometrical rigidity of the square plate of the wrinkled cross section, and the pipe wall thickness, respectively.
Once the target probability of failure is given by $p_{f,2}^{\text{Target}}$ or $p_{f,3}^{\text{Target}}$, the required critical strain is derived in the following way:

$$E\left(\varepsilon_W^2\right) = E\left(\varepsilon_p\right) + \beta_2 \sqrt{\operatorname{var}\left(\varepsilon_W^2\right) + \operatorname{var}\left(\varepsilon_p\right)} \tag{9a}$$

$$E\left(\varepsilon_W^3\right) = E(\Delta\varepsilon) + \beta_3 \sqrt{\operatorname{var}\left(\varepsilon_W^3\right) + \operatorname{var}(\Delta\varepsilon)} \tag{9b}$$

in which

$$\beta_2 = -\Phi^{-1}\left[p_{f,2}^{\text{Target}}\right], \qquad \beta_3 = -\Phi^{-1}\left[p_{f,3}^{\text{Target}}\right] \tag{10}$$

For a permanent ground displacement (PGD), the probability of failure can be estimated with the critical length producing the buckling formation as follows:

$$p_{f,PGD}^3 = P\left[\left(1 + \frac{1}{2} n\right) l_B < l_x\right] \tag{11}$$

in which l_x is a stretch of a pipeline subjected to shear force, n is the number of the wrinkles, and l_B is the critical length to produce the single wrinkle formation, which is given by

$$l_B = \frac{tE\varepsilon_W^2}{\tau_{cr}} \tag{12}$$

where τ_{cr} is the critical shear stress of the surrounding soil.

4.2. Seismic Safety Assessment for Ground Shaking

The seismic safety of arc-welded steel pipelines is assessed for Level 2 ground motion using Equations (4) and (7). The numerical conditions are summarized in Table 9. The pipe strain and the ground strain are compared with the critical strain for the buckling failure and that for the fatigue failure in Figure 9, where the critical strain for the buckling failure is 0.5% from Equation (5), and the critical strain for the fatigue failure is given by Equation (8) with $\varepsilon_{F_{cr}} = 3\%$. This numerical result shows that the maximum pipe strain of 0.135% in Fig.9 is less than these critical strains.

Table 9 Data for numerical conditions.

Item	Symbol	Unit	Value
Pipe diameter	D	mm	812.8
Pipe thickness	t	mm	7.1
Factor for buckling height	s		0.3
Pipe depth	h	m	1.2
Thickness of surface groun	H	m	50

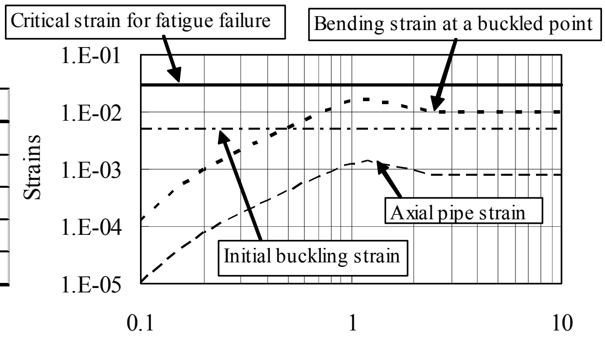

Figure 9 Ground, pipe and its corresponding strains for typical periods of ground.

4.3. Seismic Safety Assessment for the PGD

When two wrinkling layers (n=2) are superimposed, the critical interval of $(1+n/2)l_B$ is estimated as 75m. This means that, if the interval to be loaded by PGD is more than 75m, multi-layered buckling is possible. In the case of liquefaction (JGA 1998, 2004), on the other hand, in which the critical shear stress decreases by 1/10 in the normal ground condition from Equation (12), the corresponding critical interval must be ten times 75m. Since the ordinary interval of liquefaction was shorter than 100m in past earthquakes, the formation of superimposed winkling layers may be impossible in buried pipelines.
If the critical shear stress is not decreased by liquefaction, an interval shorter than 75m is not sufficient to produce such multiple wrinkling layers.

5. CONCLUSION

Based on a full-scale compression experiment, the critical strains for the repairable and ultimate limit states are derived for arc-welded steel pipelines.

The results of this research are summarized as follows:
(1) In a buckling experiment with a thin wall steel pipe of D/t=110, the simple compression mode shifts to a diamond mode under increased compression.
(2) The leakage initiation process from crack formation comprises several steps; (a) first buckling formation, (b) buckling layer formation, (c) superimposition of the buckled layers, (d) surface crack formation, and (e) through-crack formation.
(3) The repairable limit state for a steel water pipe of D/t=110 is given by the buckling initiation strain as 0.50%, and the ultimate limit state is given by the fatigue crack strain as 5%, respectively.
(4) The seismic strain for Level 2 ground motion is around 1/3 of the critical strain for buckling initiation, so wrinkling formation is difficult for the design seismic load. Even if a single wrinkle is formed, the pipe strain cannot develop to a fatigue crack.
(5) In case the critical shear stress is not decreased by the liquefaction, an interval shorter than 75m is

not sufficient to produce multiple wrinkling layers.

REFERENCES

Japan Water Works Association, (2009), Seismic design guideline of water pipelines and facilities, JWWA.

Imai, T. and T. Koike, (2010), Seismic damage prediction formula of water pipes with mechanical joints, Journal of JSCE, Group A, Vol.66, No.2, pp. 344-355.

Imai, T. and Koike, T. (2009), Seismic risk management for an existing lifeline system, ICOSSAR2009 (Osaka).

Japan Water Works Association, (1997), Seismic design guideline of water pipelines and facilities (old version), JWWA.

Japan Water Steel Pipes, (1996), Buckling experiment of water steel pipes, WSP 060-96.

Japan Gas Association, (2004), The seismic design guideline of the high pressure gas pipelines, JGA.

ASME (1997) : Boiler & Pressure Vessel Code, SectionⅢ, Division 1.

Japan Gas Association, (1998), The 1998 investigation report of the liquefaction disaster prevention project, JGA.

Japan Industrial Standard Association, (2007), Coated steel pipes of the water pipelines – Section 1 Straight pipes, JIS G 3443-1.

The Ministry of Health, Labors and Welfare (2008), The partial modification of the technical guideline of the water pipeline and facilities, 2008-MWL-60, MHLW.

Ohuchi, H., (2008), The seismic design method of the concrete structural systems, Morikita Publishing Company.

Goto, Y. and Cho, S., (1997), Inelastic bifurcation analysis from a simple to diamond buckling of thick wall shell cylinders, Proceedings of the 53rd Annual Conference of the JSCE, pp.272-273.

Kato, B. Akiyama, H. and Suzuki, H. (1973), Inelastic local buckling of steel pipes under axial compressions, The Journal of Japanese Architecture Association, No.204, pp.9-17.

Timoshenko, S.P. and Gere, G.M. (1961): Theory of Elastic Stability, Second Edition.

Bathe, K. J. (1986): Automatic Dynamic Incremental Nonlinear Analysis (ADINA), ADINA R&D, Inc. (http://www.adina.com/index.shtml)